Multi-quasiparticle states in ^{256}Rf

H. B. Jeppesen,[1] I. Dragojević,[1,2] R. M. Clark,[1] K. E. Gregorich,[1] M. N. Ali,[1,2] J. M. Allmond,[3] C. W. Beausang,[3]
D. L. Bleuel,[4] M. Cromaz,[1] M. A. Deleplanque,[1] P. A. Ellison,[1,2] P. Fallon,[1] M. A. Garcia,[1,2] J. M. Gates,[1,2] J. P. Greene,[5]
S. Gros,[1] I. Y. Lee,[1] H. L. Liu,[6] A. O. Macchiavelli,[1] S. L. Nelson,[1,2] H. Nitsche,[1,2] J. R. Pavan,[1] L. Stavsetra,[1] F. S. Stephens,[1]
M. Wiedeking,[1] R. Wyss,[7] and F. R. Xu[6]

[1]*Nuclear Science Division, Lawrence Berkeley National Laboratory, Berkeley, California 94720, USA*
[2]*Department of Chemistry, University of California, Berkeley, California 94720, USA*
[3]*Department of Physics, University of Richmond, Richmond, Virginia 23173, USA*
[4]*Lawrence Livermore National Laboratory, Livermore, California 94551, USA*
[5]*Physics Division, Argonne National Laboratory, Argonne, IL 60439, USA*
[6]*School of Physics, Peking University, Beijing 100871, People's Republic of China*
[7]*AlbaNova University Center, KTH, Royal Institute of Technology, S-104 05 Stockholm, Sweden*
(Received 7 December 2007; revised manuscript received 25 April 2008; published 6 March 2009)

Excited states in ^{256}Rf were populated via the ^{208}Pb(^{50}Ti, $2n$) fusion–evaporation reaction. Delayed γ-ray and electron decay spectroscopy was performed and three isomeric states in ^{256}Rf have been identified. A fourth low-energy nonyrast state was identified from the γ-ray decay of one of the higher lying isomers. The states are interpreted as multi-quasiparticle excitations.

A new generation of experiments on the structure and properties of the heaviest nuclei is addressing the fundamental issue of the maximum mass and charge that a nucleus can attain. (For a recent review see Ref. [1].) Of particular interest for this Rapid Communication is the study of K isomers, found in the region of prolate deformed nuclei centered near ^{252}Fm ($Z = 100$, $N = 152$) [2]. These long-lived states occur when unpaired nucleons couple their angular momenta such that the projection of the total angular momentum on the deformed symmetry axis, K, is large. Approximate conservation of the K-quantum number means that decays from high-K states to low-K states are strongly hindered. By identifying such high-K states, and studying their decay, one can learn about the single-particle structure, pairing correlations, and excitation modes of the heaviest nuclei [3–6]. In this Rapid Communication we report on an investigation of K isomerism in ^{256}Rf.

The experiment was carried out at the 88-Inch Cyclotron of the Lawrence Berkeley National Laboratory and used the Berkeley Gas-filled Separator (BGS) [7]. Excited states of ^{256}Rf were populated by the ^{208}Pb(^{50}Ti, $2n$) fusion–evaporation reaction at a beam energy of 243 MeV ($\approx$239 MeV at the center of the target). This energy corresponded to the peak of the reaction cross section [$\sigma_{max} = 17(2)$ nb] as determined from an excitation function measurement. Details of the excitation function, production mechanism and decay spectroscopy of other channels [including the observation of a new 109(13)-μs isomeric state in ^{257}Rf] will be reported elsewhere. The beam passed through a $\approx$45 μg/cm^2 thick carbon window, which separates the beamline vacuum from the He gas inside the BGS, and was incident on the $\approx$0.5 mg/cm^2 thick ^{208}Pb targets. The targets each had a $\approx$25 μg/cm^2 carbon fronting and were mounted on a rotating target wheel. The average beam intensity on target was $\approx$200 particle nA. Evaporation residues were collected by the BGS and separated from the beam and other reaction products by their differing magnetic rigidities in the He gas. The evaporation residues

passed through a Multi-Wire Proportional Counter (MWPC) before being implanted into a $\approx$1-mm-thick, 16×16 pixel, double-sided silicon strip detector (DSSD) with dimensions of 5×5 cm. A standard Clover Ge detector [8] was mounted behind the 2-mm-thick Al backplate of the BGS focal plane, at approximately 5 mm from the DSSD. Source measurements over the surface of the DSSD yielded an absolute photopeak efficiency for the Clover detector of 17% at 122 keV and 3.5% at 1 MeV.

Evaporation residues were identified by observation of a signal in the MWPC coincident with a recoil implant in the DSSD, which decays, within the same pixel, by the characteristic ground-state fission of ^{256}Rf. We collected 5400 such events in a total of $\approx$6 days of beam on target. The fit to the recoil–fission time-difference distribution [9] yields a half-life of 6.67(9) ms, consistent with the accepted value of 6.4(2) ms [10]. We found no evidence of any fission branch that could be associated with the decay of an excited isomeric state.

To identify isomeric electromagnetic decays we searched for an electron signal, within the same pixel of the DSSD as the implanted recoil, prior to the fission. The DSSD pixel serves as a calorimeter detecting several electrons, or possibly L X rays, which come from the decay through highly converted low-energy transitions below an isomer [11]. Note that the recoil implants to a depth of $\approx$5 μm in the Si and the threshold for detecting an electron burst was $\approx$100 keV. Simulations show that the efficiency of detecting an electron burst, comprising four or five conversion electrons each with an energy of $\approx$40 keV, is greater than 90%. We identified a total of 985 recoil–electron–fission (r–e–f) events. The electron sum-energy spectrum is shown in Fig. 1(a). We also detected 147 recoil–electron–electron–fission (r–e–e–f) events (i.e., events with two different electron bursts). As shown in Figs. 1(b) and 1(c), the electron sum-energy spectra are markedly different for the first and second electron decays, indicating the
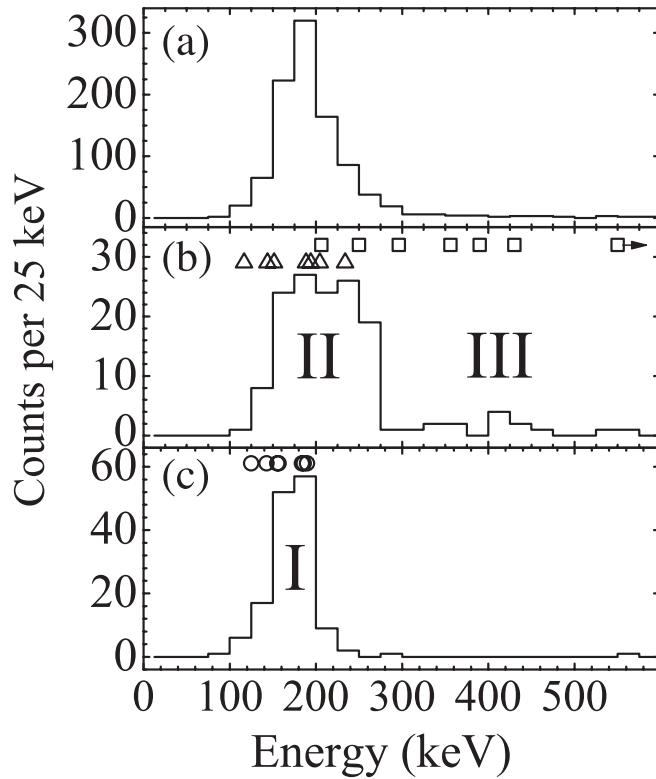
FIG. 1. Sum-energy spectrum for (a) the electrons from the r–e–f events, (b) the first electron burst from the r–e–e–f events, and (c) the second electron burst from the r–e–e–f events. The electron distributions associated with the three isomers are labeled **I**, **II**, and **III**. Open symbols indicate the sum energies for the first (squares), second (triangles), and third (circles) electron bursts in each of the seven r–e–e–e–f events.

FIG. 2. Gamma-ray spectra for (a) γ rays in prompt coincidence with electrons from the r–e–f events, (b) γ rays in prompt coincidence with the first electron burst from the r–e–e–f events, and (c) γ rays in prompt coincidence with the second electron burst from the r–e–e–f events. The inset in (a) is an expansion with the Rf X-ray energies marked. All γ-ray spectra were created by treating the four Clover crystals as individual detectors (with no addback).

presence of at least two isomeric states. There were also seven recoil–electron–electron–electron–fission (r–e–e–e–f) events. We estimate that there was a probability of less than 1 in 500 for one such random event being present in our data. Therefore, these seven events reveal the presence of a third isomer.

We searched for γ rays detected in the Ge detector in prompt coincidence (±160 ns) with the isomeric electron signals. The total γ-ray spectrum is shown in Fig. 2(a). There is a prominent peak at 900(1) keV. There are 35 counts in this peak and the spectrum has a total of 227 counts. This is consistent with the peak-to-total ratio from source measurements (14%) and we conclude that the spectrum shown in Fig. 2(a) mainly comprises a single 900-keV transition and its Compton-scattered events.

For the r–e–e–f events we can compare the γ-ray spectrum in prompt coincidence with either the first or second electron decay. These are shown in Figs. 2(b) and 2(c), respectively. It is clear that the second electron decay, corresponding to the isomer at lowest excitation energy, is in prompt coincidence with the 900-keV transition. In Fig. 1(c), we label this electron distribution **I**; it peaks at ≈175 keV with a maximum energy of around 225 keV. The first electron decay [Fig. 1(b)] has a very different γ-ray spectrum in prompt coincidence [Fig. 2(b)]. All γ rays associated with this first electron decay involve
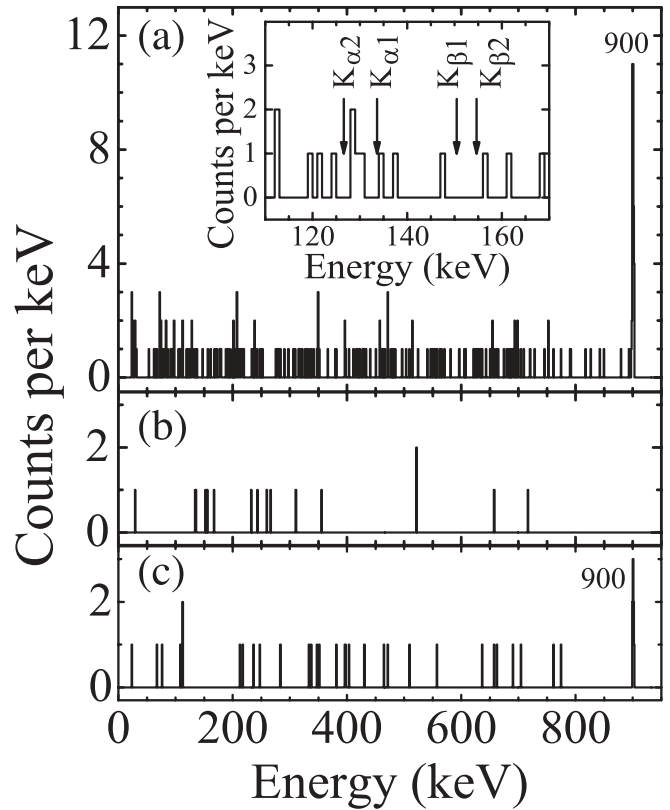
electron sum energies above 200 keV. Therefore, we identify two distinct distributions associated with the first electron decay, which we label **II** and **III** in Fig. 1(b). Distribution **II** peaks at ≈200 keV with a maximum electron sum energy of around 275 keV. Distribution **III** involves electron sum energies that peak at around ≈400 keV and extend beyond 500 keV. Electrons associated with distribution **III** can be in prompt coincidence with γ rays [shown in Fig. 2(b)]. These observations are supported by the characteristics of the r–e–e–e–f events. The positions of the electron sum energies for the first, second, and third decays in each of the seven events are marked in Fig. 1. They agree perfectly with the electron sum-energy distributions discussed earlier.

The evidence suggests three isomers with distinguishable decay characteristics. A partial level scheme is presented in Fig. 3. The isomer lowest in excitation energy is associated with electron distribution **I** [see Fig. 1(c)]. The electrons are in prompt coincidence with the 900-keV γ-ray transition [see Fig. 2(c)]. A second isomer lies ≈275 keV higher in excitation energy. We only see electrons associated with its decay, and these correspond to distribution **II** in Fig. 1(b). The third isomer lies at least 800 keV higher. This is deduced from the sum energy of the electrons [distribution **III** of Fig. 1(b)] plus the energies of the γ rays detected in prompt coincidence.
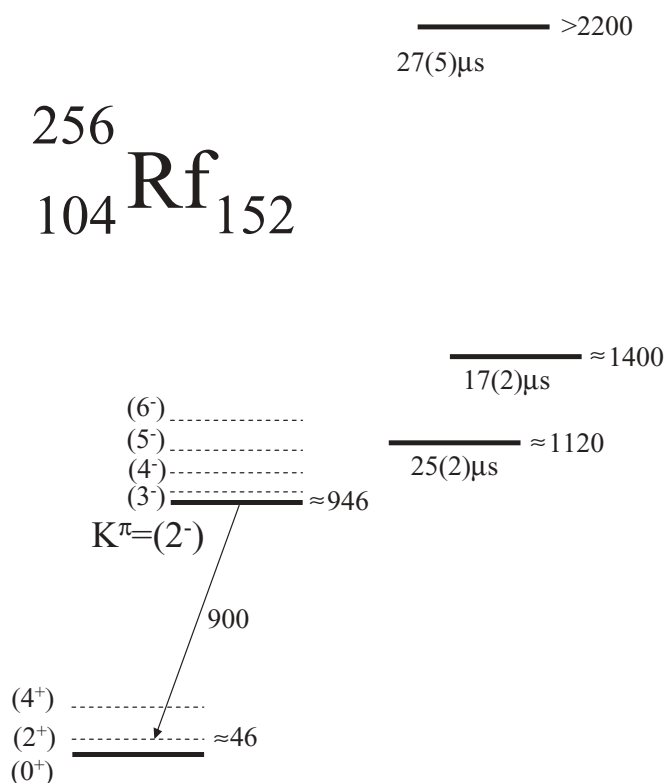
FIG. 3. Proposed decay scheme for ^{256}Rf. Energies are given in keV. Half-lives are written beneath each isomer.

FIG. 4. (Color online) The fitted decay curves derived from a maximum likelihood technique [9] for electron bursts **I**, **II**, and **III**. The thick solid lines are fits; the thin solid lines indicate the 68% Poisson probability interval about the fit.

The r–e–e–e–f events show that each of the three isomers has a half-life of ∼20 μs. It is unusual to find three isomers with very similar half-lives in the same nucleus. We have carefully examined the possibility of false correlations in our data but find no evidence of any background recoil–electron (r–e) events being recorded by the acquisition. During this same experiment we ran at several different energies for the excitation-function measurement and populated ^{257}Rf via the 1n-evaporation channel. We also performed additional experiments with similar recoil-implantation energies [^{208}Pb(^{48}Ca, 2n)^{254}No and ^{209}Bi(^{48}Ca, 2n)^{255}Lr] using the identical setup. We have identified several isomers, but the case of ^{256}Rf is the only one in which ∼20-μs isomers were discovered. This, combined with the fact that we can clearly distinguish different electron sum-energy distributions associated with the different isomers and that the different electron distributions are coincident with different γ rays, means that we are very confident in the existence of three distinct ∼20-μs isomers in ^{256}Rf.

To estimate half-lives more accurately using the r–e–f, r–e–e–f, and r–e–e–e–f events, we must account for the possibility of an isomer decaying during the ≈14-μs deadtime of the data acquisition. Different subsets of events were used to estimate the half-lives of the isomers. Decay curves are shown in Fig. 4. For the lowest isomer we used the lifetimes of (a) the third electron decay in the r–e–e–e–f events, (b) the electron decays coincident with 900-keV γ rays, and (c) the second electron decay in r–e–e–f events when the first isomer decay had a total energy of $E_{e+\gamma} < 275$ keV. The half-life
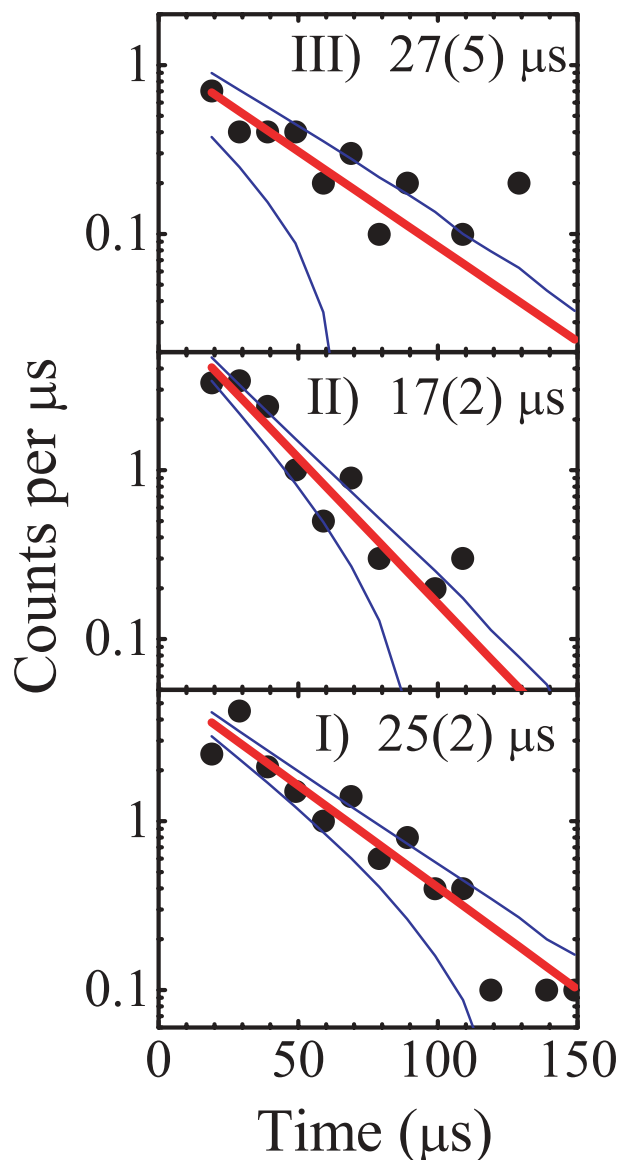
of the lowest isomer from these 158 events is 25(2) μs (see lower panel of Fig. 4). We also used the time distribution of the 35 counts in the 900-keV γ-ray peak, as seen in Fig. 2(a), to estimate the half-life of this isomer, yielding a value of 33(8) μs. For the second isomer we used (d) the second electron decay in r–e–e–e–f events and (e) the first electron decay of r–e–e–f events when this decay has a total energy of $E_{e+\gamma} < 275$ keV. The half-life of the second isomer from these 124 events is 17(2) μs (see middle panel of Fig. 4). For the highest isomer we used (f) the first electron decay in r–e–e–e–f events and (g) the first electron decay in r–e–e–f events when this decay has a total energy of $E_{e+\gamma} > 275$ keV. The half-life of the highest isomer from these 30 events is 27(5) μs (see upper panel of Fig. 4). We developed a model of the population and decay of the isomers

that provided a consistency check for our results and allowed us to estimate the probability of misassignment of electron bursts used in the half-life estimations just discussed. We find that the number of electron bursts misassigned to the decay of the lowest, middle, and highest isomer is expected to be less than 1%, 3%, and 1% of the respective totals used for the estimations.

As shown in Fig. 3, we propose that the 900-keV transition decays from a state intermediate in excitation energy between the lowest isomer and the ground state. Most of the electron sum energy is the result of decay through the low-energy transitions of the presumed rotational structure built on this intermediate bandhead. This situation is similar to that observed in recent studies of ^{252,254}No [3–5] and ^{250}Fm [6]. From X-ray intensity arguments it is possible to restrict the multipolarity of the 900-keV transition. The strongest $K_{\alpha 1}$ line has an energy of 133.4 keV, well above the detection threshold of the Clover Ge detector. If the 900-keV transition were an $M1$ transition we estimate that we should detect ≈ 17 K X rays, an $E2$ transition would yield ≈ 3, and an $E1$ transition would yield ≈ 1. Since we see no identifiable K X rays we favor an $E1$ character for the 900-keV transition.

We can restrict the angular momentum value of the state in the ground-state band populated by the 900-keV transition. Any value above $I^\pi = 4^+$ would result in observable effects such as X rays from conversion of the in-band $E2$ transitions (likely to lie above the K edge at 155 keV), a higher-than-observed upper limit of the electron sum energy, or the observation of γ rays at the energies of either the $8^+ \rightarrow 6^+$ or $6^+ \rightarrow 4^+$ ground-state band transitions. Since we do not see any of these, we conclude that the 900-keV transition is decaying to one of the lowest three states in the ground-state band.

We now consider the nature of the intermediate state, which decays via the 900-keV transition. Several lighter nuclei, including ^{252}No [5], ^{250}Fm [6], and ^{250}Cf [12], are known to have $K^\pi = 2^-$ states at low excitation energy. These states are generally interpreted as having octupole vibrational character, but microscopic calculations indicate that the configurations of such 2^- states can be dominated by a single two-quasiparticle component [13]. The decay of such a state is dominated by a strong $E1$ transition to the 2^+ level of the ground-state band. This agrees with our observation of a single strong 900-keV transition with probable $E1$ character. Systematics in the region would suggest a value of around 46(2) keV for the energy of the $2^+ \rightarrow 0^+$ ground-state band transition. This places the proposed 2^- level at an excitation energy of 946(3) keV. The isomer that feeds the rotational band based on this state can be no more than ≈ 170 keV above this level on the basis of the maximum of the observed electron sum-energy spectrum [see Fig. 1(c)]. Assuming that the band is of similar character to that observed in ^{252}No [5] and ^{250}Cf [12] this would be below the energy of the 6^- state of the excited band, or possibly even below the 5^- state. We do not see any of the in-band γ-ray transitions, which would be of low energy and highly converted. We also do not see any high-energy interband transitions, as seen in ^{252}No [5] and ^{250}Cf [12], which may reflect weaker interband decay branches in ^{256}Rf.

In the cases of ^{252}No [5] and ^{250}Fm [6] a $K^\pi = 8^-$ isomer decays to a 2^- band. The lifetimes for these $K^\pi = 8^-$ isomers

TABLE I. Calculated configurations and excitation energies of low-lying high-K two-quasiparticle states in ^{256}Rf.

K^π	Configuration	E_x (MeV)
8^-	$\nu^2([734]9/2^- \otimes [613]7/2^+)$	1.16
10^+	$\nu^2([734]9/2^- \otimes [725]11/2^-)$	1.36
7^+	$\nu^2([613]7/2^+ \otimes [624]7/2^+)$	1.66
7^-	$\pi^2([624]9/2^+ \otimes [512]5/2^-)$	1.41
8^-	$\pi^2([514]7/2^- \otimes [624]9/2^+)$	1.45
6^+	$\pi^2([514]7/2^- \otimes [512]5/2^-)$	1.53
8^+	$\pi^2([624]9/2^+ \otimes [633]7/2^+)$	1.64

are 110(10) ms and 1.93(15) s, respectively. The half-life of the isomer that decays to the 2^- band in ^{256}Rf is only 25(2) μs. The retardation of a K-forbidden transition can be estimated by its reduced hindrance expressed as $f_\nu = [(t_{1/2})_{\rm exp}/(t_{1/2})_{\rm WU}]^{1/\nu}$, where $(t_{1/2})_{\rm exp}$ is the partial γ-ray half-life, $(t_{1/2})_{\rm WU}$ is the Weisskopf estimate, $\nu = (\Delta K - \lambda)$, and λ is the transition multipolarity. We estimate f_ν values of ≈ 110 and ≈ 180 for the cases of ^{252}No and ^{250}Fm, respectively. To reproduce a similar value in ^{256}Rf, under the assumption of a dipole decay from the isomer to the 2^- band, requires that the lowest isomer in ^{256}Rf has a value of K = 6 or 7. If we assume that the second isomer also decays via a low-energy dipole transition with a similar hindrance it will have a value of K = 10–12.

As discussed earlier, the isomer with lowest excitation energy lies at ≈ 1120 keV whereas the second isomer must lie about 275 keV higher. This is the expected energy scale for several high-K two-quasiparticle states. The third isomer lies at an excitation energy > 2200 keV and may well correspond to a four-quasiparticle state. Calculations of the excitation energies of specific two-quasiparticle configurations in these nuclei are a challenge since the single-particle energies are not always well reproduced and an additional unknown arises from residual spin-spin interactions. Recent configuration-constrained Woods-Saxon potential-energy-surface calculations [14] have been relatively successful in reproducing the limited experimental data on K isomers known in nuclei with $Z \geqslant 100$. We have performed such a calculation for multi-quasiparticle states in ^{256}Rf. Active high-K proton orbitals found near the Fermi surface include the [624]9/2, [514]7/2, [633]7/2, and [512]5/2 Nilsson states. Active high-K neutron orbitals include the [734]9/2, [613]7/2, [624]7/2, and [725]11/2 Nilsson states. Calculated energies for several of the lowest possible two-quasiparticle configurations are presented in Table I. As already discussed, it is unlikely that the lowest observed isomer is based on the $\nu^2([734]9/2^- \otimes [613]7/2^+)8^-$ configuration despite being close to the predicted excitation energy. There are several other predicted states with K = 6 or 7 that might correspond to the lowest isomer. For the second isomer a probable configuration is $\nu^2([734]9/2^- \otimes [725]11/2^-)10^+$, which has the highest K value of the calculated low-lying two-quasiparticle configurations in ^{256}Rf. The high-K value of this state and the relatively low predicted excitation energy agree neatly with the deduced properties of the second isomer. Therefore, it is natural to associate the observed state with this 10^+ configuration. This would then suggest that the lower isomer is also a probable two-quasineutron state.

Our results extend to new limits, in mass and charge, the detection and spectroscopy of high-K isomeric states undergoing electromagnetic decay. Such investigations will provide stringent tests of the calculations of the structure and properties of the heaviest elements.

[1] M. Leino and F. P. Hessberger, Annu. Rev. Nucl. Part. Sci. **54**, 175 (2004).

[2] A. Ghiorso, K. Eskola, P. Eskola, and M. Nurmia, Phys. Rev. C **7**, 2032 (1973).

[3] R.-D. Herzberg *et al.*, Nature (London) **442**, 896 (2006).

[4] S. K. Tandel *et al.*, Phys. Rev. Lett. **97**, 082502 (2006).

[5] B. Sulignano *et al.*, Eur. Phys. J. A **33**, 327 (2007).

[6] P. T. Greenlees *et al.*, Nucl. Phys. **A787**, 507c (2007).

[7] C. M. Folden III, Ph.D. thesis, University of California, Berkeley, Report No. LBNL-56749, 2004.

[8] G. Duchêne *et al.*, Nucl. Instrum. Methods A **432**, 90 (1999).

[9] K. E. Gregorich, Nucl. Instrum. Methods A **302**, 135 (1991).

[10] Y. A. Akovali, Nucl. Data Sheets **87**, 287 (1999).

[11] G. D. Jones, Nucl. Instrum. Methods A **488**, 471 (2002).

[12] M. S. Freedman *et al.*, Phys. Rev. C **15**, 760 (1977).

[13] V. G. Soloviev, A. V. Sushkov, and N. Yu. Shirikova, Sov. J. Nucl. Phys. **54**, 748 (1991).

[14] F. R. Xu, E. G. Zhao, R. Wyss, and P. M. Walker, Phys. Rev. Lett. **92**, 252501 (2004).